Langmuir Article

pubs.acs.org/Langmuir

Lateral Hydrodynamic Interactions between an Emulsion Droplet and a Flat Surface Evaluated by Frictional Force Microscopy

Ivan U. Vakarelski,*[,†,∥,⊥] Raymond R. Dagastine,*[,‡] Derek Y. C. Chan,[§,#] Geoffrey W. Stevens,[‡] Ko Higashitani,[∥] and Franz Grieser[†]

[†]*Particulate Fluids Processing Centre, School of Chemistry,* [‡]*Department of Chemical and Biomolecular Engineering, and* [§]*Department of Mathematics and Statistics, University of Melbourne, Parkville, Victoria 3010, Australia,* [∥]*Department of Chemical Engineering, Kyoto University, Katsura, Nishikyo-ku, Kyoto 615-8510, Japan,* [⊥]*Institute of Chemical and Engineering Sciences, 1 Pesek Road, Jurong Island 627833, Singapore, and* [#]*Department of Mathematics, National University of Singapore, 117543 Singapore*

Received December 29, 2009. Revised Manuscript Received March 7, 2010

We introduce a lateral atomic force microscopy (AFM) method to measure the hydrodynamic drag force acting on a microscopic emulsion droplet moving parallel to a flat surface. A tetradecane oil droplet formed in an aqueous solution of sodium dodecylsulfate was attached to a V-shaped atomic force microscopy cantilever, and lateral hydrodynamic interactions between the droplet and a flat glass surface were measured using a range of scanning velocities. The droplet was positioned either far from the oscillating surface or was pressed to the surface under a constant applied load. These measurements demonstrate the feasibility of using AFM to study lateral hydrodynamic interactions and lubricity between soft matter materials relevant to a large number of applications in areas as diverse as flavor delivery in foods to the applications of emulsions or emollients in personal care products.

Introduction

Tribology has a well-developed history with a primary focus on the friction and lubrication between rigid surfaces, yet in biological systems or soft matter systems, lubricity between soft surfaces is often a key factor that determined the durability or stability of such systems. Potential areas of application range from controlling the mastication sensation of food to the perception of quality and effectiveness of emulsions or emollients in personal care products. Although lubricity between soft surfaces has been a recent focus of tribological studies with polymeric coated surfaces or biological tissues,[1−5] there are few corresponding studies that involve individual droplets or bubbles. Lateral hydrodynamic interactions between individual droplets and bubbles are involved in a number of industrial processes such as concentrated emulsions and foam flow and rheology,[15−17] deformable particle motion through thin capillaries,[18,19] and more recently in microfluidic device development,[20] but existing studies on dynamic interactions between droplets[6−11] and bubbles[12−14] are all focused on normal rather than lateral interactions. In this article, we introduce an experimental method using atomic force microscopy (AFM) that enables the measurement of the hydrodynamic force on a single emulsion droplet moving parallel to a flat surface at separations ranging from micrometers to nanometers. Developing an understanding of the lateral hydrodynamic interactions between single deformable particles is an important step toward a fundamental understanding of the behavior of multicomponent deformable particle systems.

The method developed to probe the static and dynamic interactions between particles and droplets or bubbles and the interactions between droplets and bubbles has provided significant advancements in the understanding of how hydrodynamic drainage effects couple to both the forces and the geometry of deformable interfaces. This has been possible only with the integration of the quantitative modeling and analysis of these measurments.[6−14] This report represents the initial step in the study of lateral hydrodynamic interactions. We demonstrate the feasibility of using an oil droplet immobilized on an AFM cantilever in the frictional (also referred to as lateral) mode of AFM operation to measure the hydrodynamic drag force on a droplet moving parallel to a flat surface. For a comparison to a nondeformable measurement, the lateral hydrodynamic force was measured for a large latex particle moving parallel to a flat glass surface.

*Corresponding authors. (I.U.V.) Phone + 65 6796 3880. Fax: + 65 6316 6183. E-mail: ivakarelski@gmail.com. (R.R.D.) Phone + 61 3 8344 4704. Fax: +61 3 8344 4153. E-mail: rrd@unimelb.edu.au.

(1) Yakubov, G. E.; McColl, J.; Bongaerts, J. H. H.; Ramsden, J. J. *Langmuir* **2009**, *25*, 2313.
(2) Bongaerts, J. H. H.; Day, J. R. P.; Marriott, C.; Pudney, P. D. A.; Williamson, A. M. *J. Appl. Phys.* **2008**, *104*, 014913.
(3) Stokes, J. R.; Davies, G. A. *Biorheology* **2008**, *44*, 141.
(4) Bongaerts, J. H. H.; Fourtouni, K.; Stokes, J. R. *Tribol. Int.* **2007**, *40*, 1531.
(5) Chen, M.; Briscoe, W. H.; Steven, P.; Armes, S. P.; Klein, J. *Science* **2009**, *323*, 1698.
(6) Dagastine, R. R.; Stevens, G.; Chan, D. Y. C.; Grieser, F. *J. Colloid Interface Sci.* **2004**, *273*, 339.
(7) Dagastine, R. R.; Chau, T. T.; Chan, D. Y. C.; Stevens, G. W.; Grieser, F. *Faraday Discuss.* **2005**, *129*, 111.
(8) Dagastine, R. R.; Manica, R.; Carnie, S. L.; Chan, D. Y. C.; Stevens, G. W.; Grieser, F. *Science* **2006**, *313*, 210.
(9) Manica, R.; Connor, J. N.; Dagastine, R. R.; Carnie, S. L.; Horn, R. G.; Chan, D. Y. C. *Phys. Fluids* **2008**, *20*, 032101.
(10) Webber, G. B.; Edwards, S. A.; Stevens, G. W.; Grieser, F.; Dagastine, R. R.; Chan, D. Y. C. *Soft Matter* **2008**, *4*, 1270.
(11) Webber, G. B.; Manica, R.; Edwards, S. A.; Carnie, S. L.; Stevens, G. W.; Grieser, F.; Dagastine, R. R.; Chan, D. Y. C. *J. Phys. Chem. C* **2008**, *112*, 567.
(12) Vakarelski, I. U.; Lee, J.; Dagastine, R. R.; Chan, D. Y. C.; Stevens, G. W.; Grieser, F. *Langmuir* **2008**, *24*, 603.
(13) Manor, O.; Vakarelski, I. U.; Tang, X.; O'Shea, S. J.; Stevens, G. W.; Grieser, F.; Dagastine, R. R.; Chan, D. Y. C. *Phys. Rev. Lett.* **2008**, *101*, 024501.
(14) Manor, O.; Vakarelski, I. U.; Stevens, G. W.; Grieser, F.; Dagastine, R. R.; Chan, D. Y. C. *Langmuir* **2008**, *24*, 11533.
(15) Denkov, N. D.; Tcholakova, S.; Golemanov, K.; Ananthpadmanabhan, K. P.; Lips, A. *Soft Matter* **2009**, *5*, 3389.
(16) Princen, H. M. In *Encyclopedia of Emulsion Technology*; Sjoblom, J., Ed.; Marcel Dekker: New York, 2001, p 243.
(17) Saiki, Y.; Prestidge, C. A.; Horn, R. G. *Colloids Surf., A* **2007**, *299*, 65.
(18) Bretherton, F. P. *J. Fluid Mech.* **1961**, *10*, 166.
(19) Terriac, E.; Etrillard, J.; Cantat, I. *Europhys. Lett.* **2006**, *74*, 909.
(20) Whitesides, G. M. *Nature* **2006**, *442*, 368.

The deformable droplet measurement used a tetradecane droplet stabilized with anionic surfactant sodium dodecylsulfate (SDS) immobilized on a cantilever that is moved parallel to a flat glass surface as a substrate after different degrees of droplet compression. SDS provides a repulsive static interaction force with the substrate to ensure that at a given applied normal load a stable liquid film is maintained between the deformed droplet and the substrate.[6−11] The lateral interaction forces measured under such conditions are expected to be entirely due to hydrodynamic interactions. The experimental details, including the adaptations of the lateral force microscopy method to the droplet, are presented, followed by a discussion of the results for both the latex particle and the oil droplet. This study presents the feasibility of these measurements and a qualitative analysis of these data. This is followed by a detailed discussion of some of the challenges of the quantitative analysis of the deformable droplet measurements that will be addressed in subsequent publications.

Experimental Methods

Reagents. Tetradecane oil was purchased from Fluka (99.5%+, olefine-free) and was further purified by passing through a glass column filled with an activated magnesium silicate adsorbent (Florisil). All organic reagents (ethanol, acetone, and heptane) used in cleaning the glassware, liquid cell, and samples were AR grade from Sigma-Aldrich. Octadecyltrichlorosilane (OTS, >90%, Aldrich) and sodium dodecylsulfate (SDS, >99%, Sigma-Aldrich) were used as received. Deionized water was purified using a Millipore purification system with an internal specific resistance of greater than 18.2 MΩ/cm.

Experimental Apparatus. Measurements were made using a Digital Instruments (Santa Barbara, CA) MultiMode III AFM equipped with a glass liquid cell. A schematic of the experimental setup is shown in Figure 1. A large emulsion droplet was attached below a hydrophobized V-shaped AFM cantilever. The piezotube attached to the substrate was used to oscillate it laterally to create a shear flow below the droplet that is attached to the stationary cantilever. The hydrodynamic drag on the droplet caused the cantilever to rotate, and the degree of rotation was recorded using a four-quadrant photodiode. From the lateral output signal, the torque on the cantilever was determined in a similar fashion to measurements of the frictional force using lateral force AFM measurements. The substrate was initially oscillated with the droplet far away from the surface, and then it was lowered toward the substrate using either the step motor or the piezo to measure the contribution of the droplet−substrate lateral hydrodynamic interaction. A flexible silicon O-ring seal connects the substrate to the liquid cell.

Droplet Colloidal Probe Preparation and Characterization. Emulsion oil droplets were first formed on a flat glass substrate, and then a single droplet was placed on a strongly hydrophobized V-shaped cantilever mounted in the liquid cell holder. Veeco tipless cantilevers (Veeco, NP-O) were hydrophobized by bathing in a 3 mM solution of octadecyltrichlorosilane (OTS) in heptane for 20 min and thoroughly washed with heptane, ethanol, and water.[12] The substrates were pieces of circular glass slides for the AFM liquid cell (Asylum Research). They were cleaned by washing with acetone, ethanol, and water and sonication, which resulted in hydrophilic surfaces with a water contact angle of about 20°. This cleaning procedure resulted in a surface where the oil droplets were loosely attached to the surface. Tetradecane oil droplets were initially sprayed on the center of the glass sample and covered with the SDS solution to break them into smaller droplets.[21,22] The upper portion of the

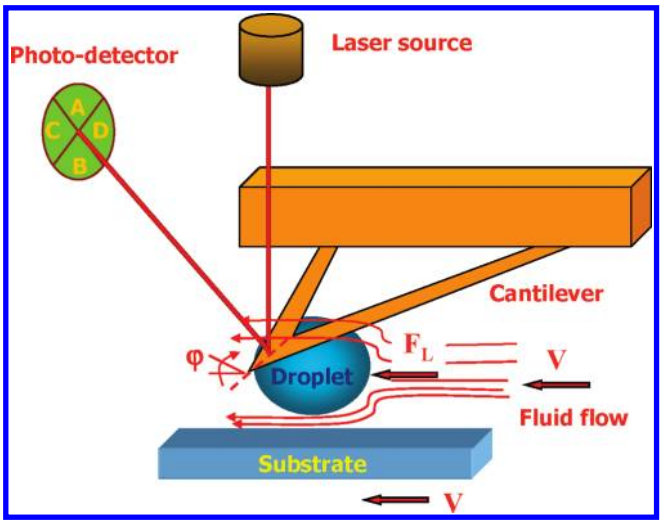

Figure 1. Schematic drawing of the experimental apparatus showing the lateral oscillatory motion of the substrate creating a shear fluid flow, V, near the surface. The hydrodynamic drag force, F_L, on the emulsion droplet causes a twisting motion of the cantilever with an angle, φ, registered by the photodetector.

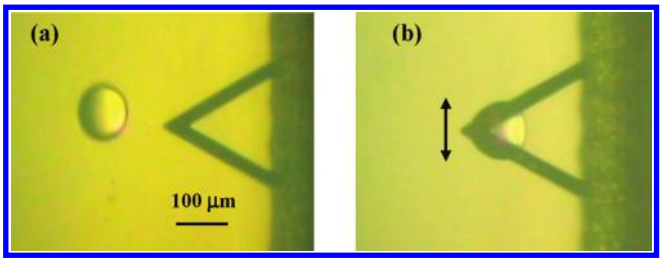

Figure 2. (a) Top microscopic view of a tetradecane oil droplet immobilized on the substrate and a V-shaped cantilever mounted in the liquid cell cantilever holder. (b) The same droplet after been pulled off of the surface onto the cantilever. The arrow indicates the substrate oscillation direction in the lateral-mode measurement experiments.

fluid cell is composed of the glass tip holder that makes a seal with the walls of the cell using a silicon O-ring. Additional solution was added, as required, to fill the entire cell volume. An optical system from above was connected to a CCD camera to monitor the cantilever position over the droplet of interest on the substrate. The droplet was transferred from the glass surface to the cantilever by pressing on the droplet with the cantilever tip and then retracting the cantilever from the surface using the step motor.[12,22,23] The process of droplet attachment is illustrated in Figure 2.

The larger area of the V-shaped cantilevers facilitated the attachment of larger emulsion droplets compared to that resulting from rectangular cantilevers usually employed in friction-force AFM measurements.[25−30] To characterize the droplet probe better after the measurements were made, we transferred the

(21) Dagastine, R. R.; Prieve, D. C.; White, L. R. . *J. Colloid Interface Sci.* **2004**, *269*, 84.
(22) Clasohm, L. Y.; Vakarelski, I. U.; Dagastine, R. R.; Chan, D. Y. C.; Stevens, G.; Grieser, F. *Langmuir* **2007**, *23*, 9335.
(23) Gunning, A. P.; Mackie, A. R.; Wilde, P. J.; Morris, V. J. *Langmuir* **2004**, *20*, 116.
(24) Vakarelski, I. U.; Toritani, A.; Nakayama, M.; Higashitani, K. *Langmuir* **2003**, *19*, 110.
(25) Bhushan, B. *Handbook of Micro/Nanotribology*; 2nd ed.; CRC Press: Boca Raton, FL, 1995.
(26) Biggs, S.; Crain, R. G.; Page, N. W. *J. Colloid Interface Sci.* **2000**, *232*, 133.
(27) Vakarelski, I. U.; Brown, S. C.; Rabinovich, Y. I.; Moudgil, B. *Langmuir* **2004**, *20*, 1724.
(28) Donose, B. C.; Vakarelski, I. U.; Higashitani, K. *Langmuir* **2005**, *21*, 1834.
(29) Taran, E.; Donose, B. C.; Vakarelski, I. U.; Higashitani, K. *J. Colloid Interface Sci.* **2006**, *297*, 199.
(30) Donose, B. C.; Taran, E.; Vakarelski, I. U.; Shinto, H.; Higashitani, K. *J. Colloid Interface Sci.* **2006**, *299*, 233.

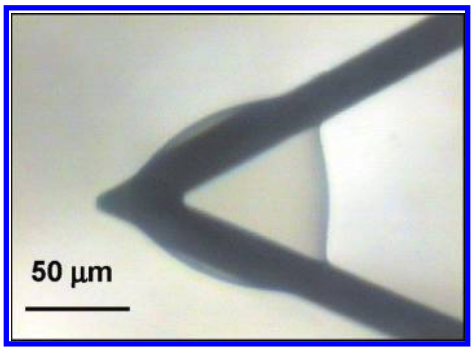

Figure 3. High-magnification top-view microscopic image of a V-shaped cantilever with an attached emulsion droplet.

probe from the AFM cell to a solution-holding Petri dish to take higher-resolution images such as the one shown in Figure 3. This type of image was used to estimate the approximate droplet dimensions (characterized by two primary radii of curvature) and also to verify that the droplet base was pinned to the hydrophobized cantilever edges. Both this study and previous studies[6,8] suggest that the pinning along the cantilever edge guaranteed the stability of the droplet attachment during the lateral measurements. For future investigations we are developing custom-designed rectangular cantilevers with an integrated coin platform at the free end that will allow for the attachment of large emulsion droplets with a well-defined, easily determined spherical shape.

Latex Particle Probes. Monosized polystyrene latex particles of 100 μm average diameter and a density of 1.05 g/cm (Duke Scientific) were attached to the end of the V-shaped cantilevers with a small amount of epoxy glue (Shell) using a micromanipulator equipped with an optical microscope. Because the polystyrene particle density is close to that of water, no significant cantilever bending was observed despite the large particle size and low cantilever spring constant.

Measurement of the Lateral Hydrodynamic Force. Prior to the lateral force measurement, force measurements normal to the surface were made following the procedures developed previously.[8,21−24] The lateral hydrodynamic interaction was then measured using frictional-force-mode AFM. This is similar in procedure to "contact friction" AFM force measurements.[25−30] In brief, in friction mode the probe (cantilever tip or solid colloidal particle) is pressed against the substrate with a constant applied load while the substrate slides in a direction perpendicular to the cantilever long axes via lateral oscillation (Figure 2b, see direction of arrow). The magnitude of the torque on the cantilever, T_L (N m), is determined from the difference in the lateral force detector signal, ΔU_L (V), during the opposite-direction scans, completing one full scan cycle or friction-force loop according to the relation

$$T_L = \frac{1}{2}\Delta U_L S_L K_L \qquad (1)$$

where S_L (rad/V) is the lateral detector sensitivity and K_L (N m/rad) is the cantilever lateral spring constant. For the case of contact or friction-force measurements, the lateral force F_L (N) is determined according to $T_L = F_L H$, where H is the distance from the cantilever to the contact point; for a particle, H is twice the radius, $H = 2R$. In the lateral hydrodynamic measurements, the particle or droplet is separated from the substrate by a thin liquid film and the force acting on the particle or droplet is distributed over the entire surface, not at a particle−substrate contact zone as in the contact friction measurements case. The conversion to lateral forces, F_L, is a more complicated process, as discussed below.

The lateral interaction forces measured were hydrodynamic in nature and much lower magnitude than in the case of solid-surface contact friction. A combination of low cantilever spring constants, large particles (oil droplet or latex particle), and high scanning rates was used to obtain sufficient sensitivity to these

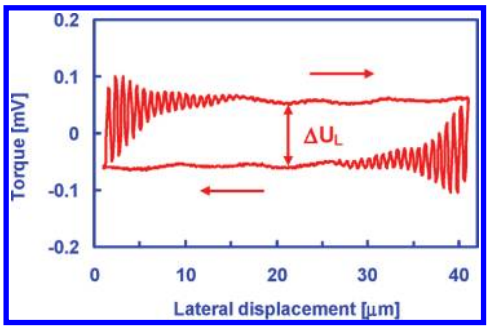

Figure 4. Typical hydrodynamic friction-force loop of lateral piezo displacement vs lateral photodiode output signal for an emulsion droplet of approximately 90 μm diameter compressed with a normal load of 40 nN and a scan velocity of 800 μm/s (40 μm scan size, 10 Hz scan frequency). The arrows show the scan direction.

weaker forces. An example for the hydrodynamic-force friction-force loop for an emulsion droplet compressed against a flat piece of glass is shown in Figure 4. Similar to the contact friction-force loop, the cantilever torque force is proportional to the difference in the lateral oscillation cycle output signal, ΔU_L. As the scan direction changes, a strong oscillation of the cantilever is visible in Figure 4. It is possible that these oscillations are due to the resonant oscillation of the piezo at high scan rates, which is known to occur in scanning-mode AFM imaging.[31] The interpretation of these oscillations is beyond the scope of this article, so we will restrict our consideration only to the ΔU_L magnitude. It should be noticed that for the probe−surface separation range investigated the turn in the cantilever twist was very well synchronized with the turn in the piezo scan direction (Figure 4). This result indicates that there was no significant phase shift between the movement of the piezo and the liquid adjacent to the surface. Reference experiments using tipless cantilevers without a particle or droplet were carried out to confirm that for the studied velocity range the lateral output signal was negligibly small compared to that of the particle- or droplet-loaded cantilevers.

Cantilever Spring and Detector Sensitivity Determination. There are a number of well-established methods of determining the AFM cantilever normal spring constant, K_N, and detector sensitivity, S_N, necessary for the conversion of the normal force data and the respective lateral spring constant, K_L, and lateral detector sensitivity, S_L, used in eq 1.[32−36] The cantilever normal spring constant was measured to be 0.06 ± 0.01 N/m using the Cleveland method,[34] and a scaling was used on the basis of ref 33 for the large offset nature of the droplet or sphere. The lateral spring constant was evaluated by pushing the latex particle probes against a vertically mounted cantilever with a known spring constant.[33] For the latex particle probes, lateral spring constant values were in the range of 2.0 to 3.0 nNm/rad depending on the particle loading position with a corresponding lateral detector sensitivity of $S_L = 3.4 \times 10^{-4}$ rad/V.[36] A value of 3.0 nNm/rad was taken for 90-μm-diameter emulsion droplet probe data presented in the Experimental Methods section on the basis of a latex particle probe with a similar offset.

Results and Discussion

Latex Particle Experiments. The solid spherical particle experiments employed 100-μm-diameter latex particles as colloidal

(31) Schwarz, U. D.; Koster, P.; Wiesendanger, R. *Rev. Sci. Instrum.* **1996**, *67*, 2560.
(32) Butt, H.-J.; Cappella, B.; Kappl, M. *Surf. Sci. Rep.* **2005**, *59*, 1.
(33) Vakarelski, I. U.; Edwards, S. A.; Dagastine, R. R.; Chan, D. Y. C.; Stevens, G. W.; Grieser, F. *Rev. Sci. Instrum.* **2007**, *78*, 116102.
(34) Cleveland, J. P.; Manne, S.; Bocker, D.; Hansma, P. K. *Rev. Sci. Instrum.* **1993**, *64*, 1.
(35) Neumeister, J. M.; Ducker, W. A. *Rev. Sci. Instrum.* **1994**, *65*, 2527.
(36) Bogdanovic, G.; Meurk, A.; Rutland, M. W. *Colloids Surf., B* **2000**, *19*, 397.

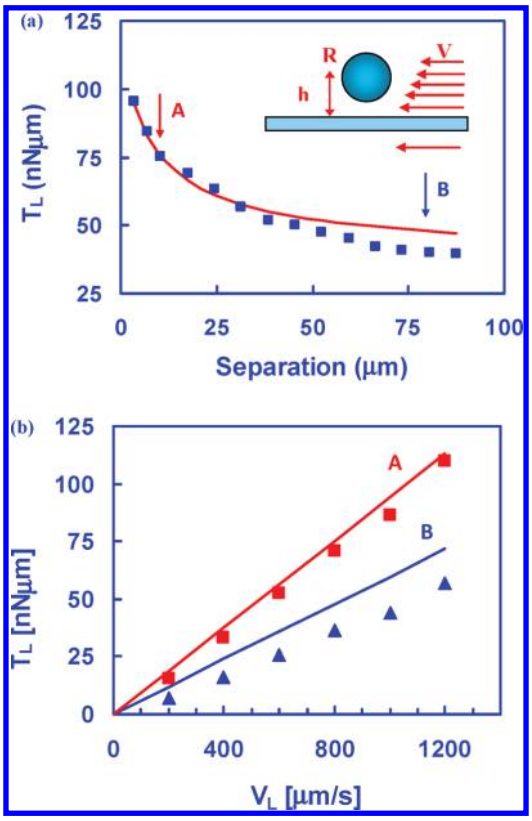

Figure 5. (a) Torque on a latex particle with a diameter of $2R$ = 100 μm as a function of the particle−surface separation ($h-R$) at a fixed lateral scan velocity of V_L = 800 μm/s. The solid red line represents the Faxen solution (eq 2). (b) Torque on the cantilever, T_L, vs the lateral scan velocity, V_L, for fixed particle−surface separations of 10 μm (red squares) and 80 μm (blue triangles). The solid lines represent the Faxen solution at each particle−surface separation. The arrows in plot a mark the positions of the corresponding data set in plot b.

probes. Typical experimental results obtained with one of the probes are summarized in Figure 5. In these measurements, the separation between the particle and the surface was regulated using the step motor function of the Multimode software control. In Figure 5a, we show the dependence of T_L, the torque due to the lateral hydrodynamic drag on the particle as a function of the particle−surface separation at a fixed lateral scan velocity of V_L = 800 μm/s. In Figure 5b, we present T_L versus V_L data for fixed separations of approximately 10 and 80 μm. The linear dependence of the torque on the scan velocity is consistent with a lateral hydrodynamic interaction controlling the torque on the cantilever. Similar scan velocity dependencies were obtained using a lateral scan size of 10 to 40 μm, but for consistency, we present data using a 40 μm scan size. Measurements were repeated using several different latex particles, and all show similar behavior within a variance of 20%. The solid lines in Figure 5a,b are formal fits of the experimental torque values to the Faxen approximation[38] of the Stokes force on a sphere moving parallel to a flat surface

$$\frac{F_L}{6\pi\mu RV} = \frac{1}{\left(1 - \frac{9R}{16h} + \frac{1R^3}{8h^3} - \frac{45R^4}{256h^4} - \frac{R^5}{16h^5}\right)} \qquad (2)$$

where μ is the liquid viscosity and h is the distance between the center of the sphere and the substrate (Figure 5a inset).

The Faxen solution is used for a rough comparison with experimental data. To calculate the lateral force acting on the cantilever from the torque measured in the AFM experiment, the distance from the sphere loading position to the cantilever is required. For frictional measurements, this is $H = 2R$ as discussed above. In the case of lateral hydrodynamic interactions, the applied lateral load is distributed across the entire sphere, thus the calculation of the force is more complicated, requiring a knowledge of the shear field as a function of the distance from the surface, accounting for the presence of the cantilever and the rotation of the particle. For purposes of comparison, we assume the contribution from the cantilever to the shear field to be small. The Faxen solution is valid for the translational motion of a sphere, which in this case is well satisfied by the small values of the cantilever rotation during the measurements. Finally, the comparison in Figure 5a assumes that the center of the hydrodynamic force acting on the sphere coincides with the center of the sphere or that $H = R$ and $T_L = RF_L$. This assumption is reasonable when the sphere is far away from the surface, but as the sphere approaches the surface, the frame of reference for the center of the hydrodynamic force moves from the center of the sphere. The contribution of the film between the particle and the wall to the hydrodynamic force affects the drag distribution over the sphere surface. This leads to an offset in the center of the drag force such that $H = (R + x) > R$, where x is the center of force with respect to the center of the sphere. Using a numerical solution[37] or the Faxen approximation,[38] we estimate that for the $h/R > 1.05$ value range presented in Figure 5 this effect is likely to be small, or $x/R \ll 1$.

The gradual deviation in the Faxen solution for separation distances > 50 μm could be due to a decrease in the liquid velocity away from the surface because of the finite size of the liquid cell. Strictly speaking, the sphere is moving in a shear flow where the velocity of the liquid adjacent to the substrate is equal to the piezo scan velocity and gradually decreases to zero at the top of the fluid cell. The thickness of the fluid cell is about 1000 μm, and there is a linear shear flow profile between the substrate and the top of the fluid cell. Thus, the assumption that the deviation at larger separations is due to a decrease in the velocity flow field is reasonable. In the range of separation distances 0 to 50 μm from the surface relevant to the measurements, for the emulsion droplet experiments (Figure 6), the assumption of a constant velocity flow field matching the velocity of the piezo scanner velocity, V_L, is reasonable. The size of the O-ring is approximately 1 cm in diameter and the lateral scan size ranges from 10 to 40 μm, thus the O-ring is not expected to perturb the flow field around the sphere.

Considering limitations discussed above, the good experimental agreement with the Faxen solution suggests the generally consistent measurement of the lateral hydrodynamic force in the proximity of the substrate. Previous measurements of the drag forces on micrometer-sized particles in the vicinity of a flat surface were studied by Schäffer et al.[39,40] using an optical tweezers method. In addition, Benmouna and Johannsmann[41] measured the Brownian motion of an AFM colloidal probe near an inclined wall. Although these measurements allow for more rigorous comparisons to theoretical results by Faxen[38] or Brenner,[37] they do not allow for the study of the deformation of a droplet under compression near a flat surface.

(37) Goldman, A. J.; Cox, R. G.; Brenner, H. *Chem. Eng. Sci.* **1967**, *22*, 637.
(38) Faxen, H. *Ark. Mat., Astron. Fys.* **1923**, *17*, 1.
(39) Tolić-Nørrelykke, S. F.; Schäffer, E.; Howard, J.; Pavone, F. S.; Jülicher, F.; Flyvbjerg, H. *Rev. Sci. Instrum.* **2006**, *77*, 103101.
(40) Schäffer, E.; Tolić-Nørrelykke, S. F.; Howard, J. *Langmuir* **2007**, *23*, 3654.
(41) Benmouna, F.; Johannsmann, D. *J. Phys.: Condens. Matter* **2003**, *15*, 3003.

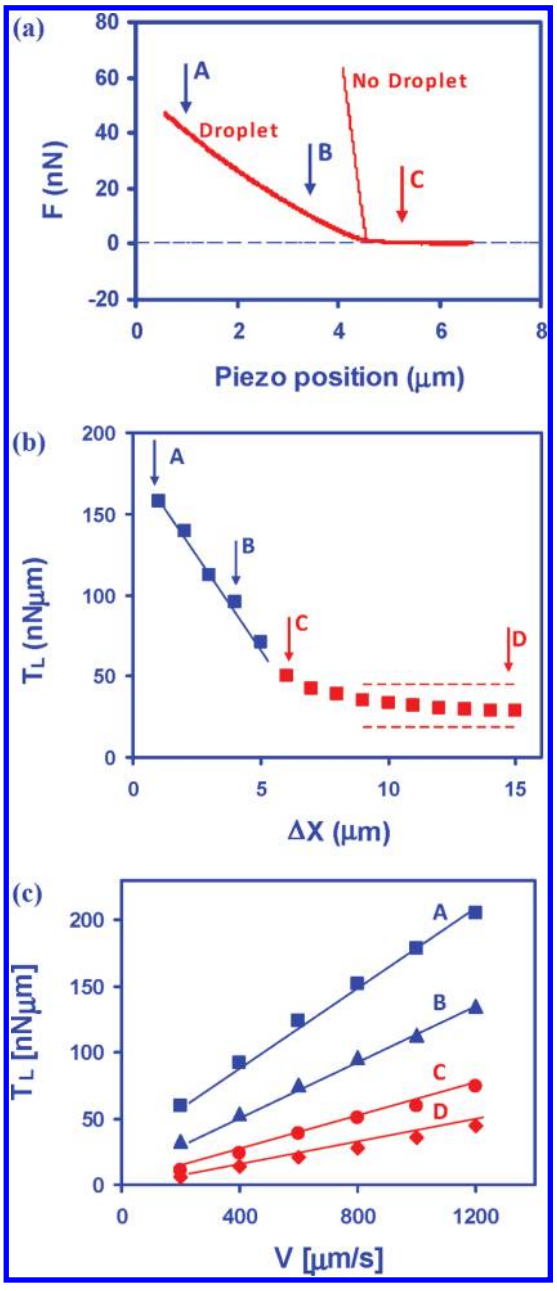

Figure 6. (a) Approach curve of the normal interaction force, F, vs the relevant piezo position for a 90 μm (average diameter) tetradecane droplet immobilized on a cantilever pressed against a glass surface in 10 mM SDS solution (solid line) compared to an approach force curve for a cantilever without an immobilized droplet pressed against a rigid surface (thin line). (b) Cantilever lateral torque, T_L, vs piezo position for the same droplet oscillating with a constant scan velocity of $V_L = 800\,\mu$m/s. Red squares are for the droplet oscillating above the surface without compression, and blue squares are for the compressed droplet. The dashed red lines are the torque calculated from the Stokes drag force of spherical particles with diameters of $2R = 70\,\mu$m (lower line) and $2R = 110\,\mu$m (upper line). (c) Cantilever lateral torque, T_L, vs lateral scan velocity, V_L, where data sets correspond to (from the lowest to the higher) a droplet−surface separation of approximately 10 μm (red diamonds), a droplet−surface separation of approximately 1 μm (red circles), the droplet compressed under a normal load of $F = 10$ nN (blue triangles), and the droplet compressed under a normal load of $F = 40$ nN (blue squares). The arrows in plots a and b mark the positions of the corresponding data sets in plot c.

Emulsion Droplet Experiment. We present the torque on the cantilever that arises from the lateral hydrodynamic drag force between a tetradecane emulsion droplet immobilized on a cantilever and a flat glass surface in a solution of 10 mM SDS. The droplet shape and dimensions were close to that of the droplet shown in Figure 3 with an average droplet diameter of 90 μm. The normal interaction force curve during the droplet compression toward the surface as the force versus relative piezo position change is presented in Figure 6a. These data were collected at an approach velocity of 1 μm/s where the effects from hydrodynamic forces were negligible compared to the magnitude of the force.[6,22] A force curve between a cantilever without an immobilized droplet and the flat surface is shown in the same Figure. Quantitatively describing the deformation of the droplet requires a detailed analysis,[8] but a simple estimate of droplet deformation at high force loads can be made if the expected film thickness is much less than the magnitude of the deformation. In this case, the difference in the deflection between the cantilever without an immobilized droplet and the droplet-loaded cantilever can be used to estimate the static droplet deformation, h_0. If the expected film thickness is nonzero but satisfies the condition $d_0 \ll h_0$ (notation in Figure 7), then the deformation can be computed from a simple distance balance given by

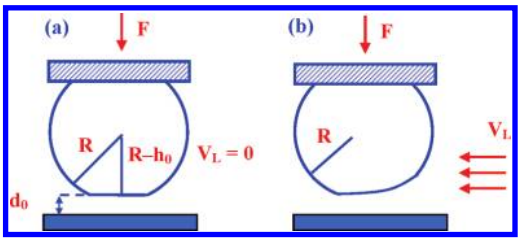

Figure 7. Schematic drawing of an emulsion droplet compressed with a normal force F to the surface: (a) no shear flow is applied and (b) schematic droplet profile change with the shear flow applied.

$$h_0 = \Delta l_0 - d_N \tag{3}$$

where Δl_0 is the change in piezo motion after the contact point defined by the cantilever force curve without an immobilized droplet and $d_N = F_N/K_N$ is the cantilever deflection.

In the case of a nondeformed droplet at large separation distances from the surface, the change in the piezo motion is equal to the change in the surface−droplet separation. The determination of the droplet−surface separation during the lateral shear measurement will require the development of a theoretical model relating the droplet shape to the system principle parameters similar to the previous modeling approach for normal droplet interactions.[8−11]

The effects of piezo position and scan velocity on lateral torque on the cantilever, T_L, calculated from the lateral output signal, ΔU_L, following eq 1 on the same droplet are shown in Figure 6b,c. In Figure 6b, we present the torque as a function of changing the piezo position in the z direction at a fixed lateral scan velocity of $V_L = 800\,\mu$m/s. In Figure 6c, we show the torque as a function of the lateral scan velocity, V_L, at several fixed piezo positions. In both plots, the droplet was initially compressed to the point of the onset of the measured force in the normal direction and then was withdrawn 10 μm from the surface using the step motor. The droplet was then stepped toward the surface in 1 μm increments, taking lateral measurements at fixed piezo positions. As shown in Figure 6b, once the piezo position corresponding to the rise in the normal force measurements was reached, a further 5 μm of piezo translation toward the substrate was used. The compression of the droplet increased rapidly, as did the corresponding lateral hydrodynamic interactions. The lateral hydrodynamic response is

shown as a function of the lateral scan velocity for four different fixed piezo positions in Figure 6c. The first two separations include no or little droplet compression corresponding to 10 μm above the surface or just above the surface or a separation of less than 1 μm, at which the normal droplet−surface interaction was still negligible. The remaining two separation distances are incorporated droplet compressions with the substrate at constant applied loads of 10 and 40 nN. Arrows in Figure 6a,b mark the relevant piezo positions at which the constant load data in Figure 6c were taken.

The drag force on the droplet above a freely oscillating surface is compared to the Stokes drag force of a solid particle with similar dimensions to a rough order-of-magnitude estimate for these data. The dashed lines in Figure 6b correspond to the torque on a particle from the Stokes drag force (e.g., $T_L = RF_L = 6\pi\mu R^2 V_L$) for particles with lower and upper limits for the characteristic droplet dimensions, $2R = 70$ and 110 μm. The general agreement suggests that effects from surfactant transport on the oil−water interface are minimal. This observation is consistent with previous studies on the normal hydrodynamic interactions between droplets under identical solution conditions (10 mM SDS) where the immobile surface or nonslip boundary condition is well satisfied at the emulsion droplet interface.[8−11]

The approximate comparisons confirm that these torque data correspond to a reasonable range for the drag force measured on an emulsion droplet. As the droplet approaches the surface, there is a gradual increase in the torque similar to that for the solid-particle case shown in Figure 4a. In Figure 5b, the torque increases gradually at lower applied loads. However, once a significant load is applied to the droplet there is a sharp increase in the torque caused by an increase in the drag force. These behaviors are reflective of two competing effects associated with deformable droplets. First, as the droplet deforms, the thickness of the film between the substrate and the droplet is limited to a much larger thickness than for an equivalently sized rigid sphere, thus limiting the lateral drag to a lower force than for a rigid system. However, as higher loads are applied to the droplet, the radial dimensions of the film grow, creating a larger interaction area and increasing the lateral drag force.

A more quantitative discussion of these data is limited by the complexity of the geometry. The analytical models developed to describe the normal hydrodynamic interactions take advantage of the axisymmetric geometry, showing the intercoupling of the geometry of the interface to the hydrodynamic drainage behavior between the droplet and the surfaces.[8] As depicted in Figure 7, the problem no longer has the same convenient symmetry. In addition, the normal drainage problem used Reynolds's lubrication where the force is dependent on the thin film region between the droplet and the substrate, but in this case, the lateral interaction force is dependent on the entire immobilized droplet, leading to a significant deformation over a large region of the droplet schematically shown in Figure 7b. A prior theoretical analysis has been suggested by Denkov[15] and co-workers on the basis of infinitely long droplets or bubbles translating above a surface, but this analysis neglects the 3D geometry of the droplet that is expected to have a significant effect on the quantitative estimate of the lateral hydrodynamic interaction.

Conclusions

We have investigated the applicability of frictional force microscopy to measure the lateral hydrodynamic forces between an emulsion droplet and a flat surface. By using a combination of relevantly large emulsion droplets (80 to 100 μm) and a low spring constant cantilever, we were able to achieve sufficient sensitivity to probe the lateral hydrodynamic drag on droplets oscillating near a flat surface within the AFM scan velocity range of 200−1200 μm/s. Despite the difficulties encountered in quantitative analysis, these results demonstrate that the relative length scales of the lateral hydrodynamic interaction span from the micrometer to the nanometer scale and that the magnitude of the force for deformable surfaces is similar to that of rigid systems. As discussed above, the nature of the deformable surface can regulate the film thickness, reducing the contribution of the thin film between the droplet and the surfaces to the drag force compared to a rigid sphere. However, the large growth in the interaction area compared to that of a rigid surface can increase the lateral hydrodynamic interaction greatly compared to that of a rigid surface. Future work in this area will focus on improved experimental methods using custom-designed cantilevers that we have recently used to study hydrodynamic interactions between bubbles.[13,14] Theoretical development will be focused on the development of a comprehensive model for data interpretation that could relate the measured lateral force versus the applied load and scan velocity dependencies to principal system parameters such as the droplet radius, interfacial tension, liquid viscosity, and surface separation.

Acknowledgment. This work is supported in part by the Australian Research Council through funding of the Particulate Fluids Processing Centre and the Australian Minerals Science Research Institute. We also acknowledge the financial support of the Core-to-Core Program promoted by the Japan Society for the Promotion of Science (project no. 18004).